Tablet Fragmentation without a Disintegrant: A Novel Design Approach for Accelerating Disintegration and Drug Release from 3D Printed Cellulosic Tablets

Basel Arafat[1,2], Magdalena Wojsz[1,3], Abdullah Isreb[1], Robert T Forbes[1], Mohammad Isreb[4], Waqar Ahmed[5], Tawfiq Arafat[6], Mohamed A Alhnan[1]*

[1] School of Pharmacy and Biomedical Sciences, University of Central Lancashire, Preston, Lancashire, UK

[2]Faculty of Medical Sciences and Public Health, Anglia Ruskin University, Chelmsford, UK.

[3]Faculty of Pharmacy with the Laboratory Medicine Division, Medical University of Warsaw, Warsaw, Poland

[4]School of Pharmacy, University of Bradford, Richmond Road, Bradford, UK

[5] College of Science/School of Mathematics and Physics, University of Lincoln, Brayford Pool, Lincoln, Lincolnshire, UK

[6] Faculty of Pharmacy and Medical Sciences, Petra University, Amman, Jordan

*Corresponding author: MAlbedAlhnan@uclan.ac.uk

University of Central Lancashire, MB025 Maudland Building, Preston PR1 2HE, UK

Tel: +44 (0)1772 893590, Fax: +44 (0)1772 892929

A B S T R A C T

Fused deposition modelling (FDM) 3D printing has shown the most immediate potential for on-demand dose personalisation to suit particular patient's needs. However, FDM 3D printing often involves employing a relatively large molecular weight thermoplastic polymer and results in extended release pattern. It is therefore essential to fast-track drug release from the 3D printed objects. This work employed an innovative design approach of tablets with unique built-in gaps (Gaplets) with the aim of accelerating drug release. The novel tablet design is composed of 9 repeating units (blocks) connected with 3 bridges to allow the generation of 8 gaps. The impact of size of the block, the number of bridges and the spacing between different blocks were investigated. Increasing the inter-block spaces reduced mechanical resistance of the unit, however, tablets continued to meet pharmacopeial standards for tablet's friability. Upon introduction into gastric medium, 1 mm spaces tablet broke into mini-structures within 4 min and met the USP criteria of immediate release products (86.7% drug release at 30 min). Real-time ultraviolet (UV) imaging indicated that the cellulosic matrix has expanded due to swelling of HPC upon introduction to dissolution medium. This was followed by a steady erosion of the polymeric matrix at a rate of 8 μm/min. The design approach was more efficient than formulation approach of adding disintegrants to accelerate tablet disintegration and drug release. This work provides a unique example where computer-aided design was instrumental at modifying the performance of solid dosage forms. Such an example may serve as a foundation for a new generation of dosage forms with complicated geometric structures to achieve functionality that are usually reached by formulation approach.

1. Introduction

With the increased focus on personalised patient treatment, the search for methods that offer flexibility in the customization of dosage forms is in high demand. Three-dimensional (3D) printing technologies provide a tool for tailoring dosage forms and are strongly paving their way into the future of oral drug delivery. Indeed, 3D printing technologies have the ability to fabricate designs and complex geometries that were not possible with traditionally manufactured dosage forms. This highly attractive technology has the capability of creating hollow or partially filled designs as well as the creation of constructs with complex drug release profiles (Alhnan et al., 2016; Goole and Amighi, 2016; Lam et al., 2002). This ability has been exploited to fabricate tablets with dual, pulsatory and/or immediate-extended release profiles (Rowe et al., 2000).

Despite the many attractive properties of the 3D printing technologies, fused deposition modelling (FDM) in particular, seems to hold more potential due to its capability in fabricating mechanically stable tablets at low cost without post-processing processes (Goyanes et al., 2015; Skowyra et al., 2015) or specialised powder facilities (Alhnan et al., 2016). Nonetheless, this technology is hindered by the elevated temperatures required for its operation as well as the restricted number of eroding polymers with thermoplastic properties suitable for FDM 3D printing (Goyanes et al., 2015; Skowyra et al., 2015). To address these limitations, research efforts to apply FDM 3D printing to different pharmaceutical grade polymers such as polyvinylpyrrolidone (Okwuosa et al., 2016), methacrylate (Sadia et al., 2016) and cellulose based polymers (Goyanes et al., 2017; Skowyra et al., 2015; Zhang et al., 2017) have been recently reported.

As the use of a thermoplastic polymer with a relatively high glass transition temperature is a pre-requisite for a successful and complete FDM 3D printing process, the resultant structures have often incorporated relatively high molecular weight polymers to yield a polymeric matrix resulting in extended drug release patterns (Goyanes et al., 2014; Goyanes et al., 2015; Skowyra et al., 2015). Due to the importance of the immediate release market, holding 70% of total oral tablet market share (GBIResearch, 2012; Marketsandmarkets, 2013) and the high safety profile of cellulosic polymers e.g. hydroxypropyl cellulose (HPC) in the pharmaceutical and food industry, it is therefore of major interest to craft an immediate release tablet out of this widely used pharmaceutical grade polymer.

Several researchers have exploited a design approach to modify drug release from a 3D printed structure. Sun and Soh (2015) modified matrix shape to achieve increasing, decreasing, constant or pulsed release of an entrapped dye. The geometric shape of the 3D printed tablet also appeared to influence to some degree the pattern of in vitro drug release (Goyanes et al., 2015). Moreover, employing different infill percentage in the 3D printed structure is another approach to modify drug release. However, this approach often results in a low density floating structures and does not accelerate drug release to an extent that meets the compendial expectations of immediate release products (Goyanes et al., 2014; Kyobula et al., 2017; Tagami et al., 2017).

In this study, a novel design approach (Gaplet) for accelerating drug release from FDM 3D printed cellulosic tablets is presented. The approach is based on utilising FDM's capability to construct relatively complex geometry designs that deliver a collapsible tablet structure. The tablets were made using the novel concept of interconnected blocks to generate intra-tablet gaps with the aim of rapid fragmentation within minutes on exposure to a dissolution medium. According to the authors' knowledge, this is the first work successfully detailing such a design concept in 3D-printed dosage forms.

2. Materials and methods

2.1 Materials

Theophylline was purchased from Arcos (United Kingdom (UK)). Hydroxypropyl cellulose (SSL grade) was provided by Nisso Chemical Europe GmbH (Dusseldorf, Germany). Triacetin was supplied by Sigma–Aldrich (UK). Sodium starch glycolate (Primojel® and Explotab®) were donated by DFE Pharma (Germany) and JRS pharma LP (United States of America (USA)) respectively. Croscarmellose sodium grades (Ac-Di-Sol® and Primellose®) were provided by FMC Biopolymer (USA) and DFE Pharma (Germany) respectively. Crospovidone (Polyplasdone™ XL-10) was donated by Ashland (USA).

2.2 Preparation and optimisation of filaments via hot-melt extrusion (HME)

A twin-screw hot melt extruder (Thermo Scientific™ HAAKE™ MiniCTW, Karlsruhe, Germany) was employed to produce a filament as a feed for the 3D printer. The compositions of the mixtures of drug, polymer and plasticizer were adapted and modified from a previous trial (Skowyra et al., 2015). Briefly, 12 g of theophylline, HPC-SSL and triacetin blend at a

weight ratio of (50:45:5) was accurately weighed and added gradually to the counter flow twin-screw extruder. The molten mass was homogenised for a minimum of 5 min at a rotation speed of 80 rpm to allow consistent distribution of the drug and the polymer. The specific temperature of initial feeding extrusion and extrusion was 120 °C. Extrusion was carried out through a 1.7 mm die nozzle with using a torque control of 0.8 Nm. Filaments were stored in sealed plastic bags at room temperature and were used as a feed for FDM 3D printing within 3 weeks of manufacture. To assess the effect of disintegrants on the formulations, Ac-Di-Sol®, Explotab®, Primojel®, Polyplasdone ™ XL-10 were added individually to the powder mixture at a weight ratio of (45:45:5:5) for theophylline, HPC-SSL, triacetin and the disintegrant.

2.3 Design and printing of tablets

A Makerbot Replicator® 2X Experimental 3D printer (Makerbot Industries, LLC, New York, USA) has been utilized to fabricate the 3D printed tablets from the HME based filament. Prototypes of product designs were developed with computer-aided design (CAD) software, Autodesk® 3ds Max Design 2016 software version 18.0 (Autodesk, Inc., USA). The obtained files were converted into a printer-readable format and imported to the printer's software (Makerbot Desktop version 2.4.0.17 Makerbot Industries, LLC, New York, USA) in an STL format. Tablets were printed using modified settings of the software for PLA filament as follows: type of printer: Replicator 2X; type of filament: PLA; resolution: standard; the speed material flow from extruder: 70 mm/s, speed of extruder travelling: 150 mm/s while traveling; infill: 100%; printer's nozzle size: 0.4 mm, height of the layer: 300 µm. To obviate the need of a post-print finishing step, tablets were printed without the use of supports or rafts.

The novel design (Gaplet) is a jointed system, developed by crafting tablets in a capsule-like structure divided into nine blocks with determined 8 spaces in between **(**Figs. 1a, b**)**. Initially, 3 sets of tablets with block widths: 0.5, 1 or 1.5 mm were designed. Each set were printed with increasing inter-block spaces: 0, 0.2, 0.4, 0.6, 0.8, 1.0 or 1.2 mm **(**Fig. 1c). The blocks within each tablet were constructed with three bridges (600 µm) connecting the blocks. The resolution was set at a layer thickness of 0.3 mm. The theoretical dimensions, volume, surface area and volume of these designs as reported by Autodesk® 3ds Max Design 2016 software are available in Table 1.

2.4 Thermal analysis

Samples (raw materials, extruded filaments and printed tablets) were characterised using differential scanning calorimetry (DSC) and thermogravimetric analysis (TGA).

For DSC analysis, a differential scanning calorimeter DSC Q2000 (TA Instruments, Elstree, Hertfordshire, UK) with a heating rate of 10 °C/min was used. Samples were heated to 100 °C for 5 min to exclude the effect of humidity then cooled to −20 °C. This was followed by a heat scan from −20 to 300 °C. Analysis was carried out under a purge of nitrogen (50 mL/min). The data was analysed using TA 2000 analysis software. Standard 40-µL TA aluminium pans and pin-holed lids were used with an approximate sample mass of 5 mg. All measurements were carried out in triplicates.

For TGA analysis, raw materials, extruded filaments and 3D printed tablets were measured using a TGA Q500 (TA Instruments, Hertfordshire, UK). Samples (5 mg) were placed in 40 µL aluminium pans and were scanned from 25 to 500 °C at a heating rate of 10 °C/min. The thermal decomposition (or degradation) profile was analysed using STARE software version 9.00. The experiments were carried out under a nitrogen gas flow of 50 mL/min. All measurements were carried out in triplicates.

2.5 X-ray powder diffraction (XRD)

A powder X-ray diffractometer, D2 Phaser with Lynxeye (Bruker, Germany) was used to assess the physical form of theophylline in the drug loaded tablets. Samples were scanned from 2Theta = 5° to 50° using 0.01° step width and a 1 sec time count. The divergence slit was 1 mm and the scatter slit 0.6 mm. The wavelength of the X-ray was 0.154 nm using Cu source and a voltage of 30 kV. Filament emission was 10 mA using a scan type coupled with a two-theta/theta scintillation counter over 30 min.

2.6 Scanning Electron Microscopy (SEM)

The surface morphology of the printed tablets was assessed using a Quanta-200 SEM microscope at 20 kV. All samples were placed on a metallic stub and gold plated using a JFC-1200 Fine Coater (Jeol, Tokyo, Japan). Photographs of the tablets were captured with a Canon EOS-1D Mark IV (Canon Ltd, Japan). Digital photographs of the 3D printed tablets were acquired, using a Canon™ EOS 100D digital camera with EF-S 18-55 mm lens.

2.7 X-ray micro-computed tomography (XµCT)

A Skyscan µCT 1272 (Skyscan, Kontich, Belgium) was used for the morphological analysis of the 3D printed Gaplets (Whole) (parameters: source voltage = 52 kV, source current = 85 µA, and image pixel size = 4.3 µm, 360º of rotation). NRecon software (version 1.6.9.8; Bruker µCT) was used for the reconstruction of the images, whilst DataViewer (Version 1.4.4; Bruker µCT) and CTVox (version 2.6.0; Bruker µCT) software were used to process the images datasets and to produce the virtual slices.

2.8 Mechanical property of the tablet.

a. Crushing strength: To evaluate the impact of the built-in gap design on the mechanical resistance of 3D printed tablets; a crushing strength tester (200 Tablet Hardness Tester, Agilent Technologies) was employed. The measured forces were intended to characterize a tablet's resistance to crushing. The tablet's long axis was oriented in the same direction of force application in the crushing strength tester. Measurements were carried out in triplicate.

b. Friability test: In order to assess the suitability of the tablet for daily handling and packaging, a friability test has been conducted. Tablets (20 units) were accurately weighed, placed in the apparatus drum (Agilent Dual-drum Friability Tester 250, Agilent Technologies) and rotated 100 times at rotation speed of 25 round/min.

c. Tensile strength test: An Instron® 5569 tensile tester (Illinois Tool Works Inc., US) was employed to study the tensile strength of the tablets. Scanning was performed under extension mode to calculate the tensile strength. Tensile strength was measured at room temperature (21 °C) and relative humidity of 50%. Samples were measured using circular geometry with data collection interval of 0.05 sec. Sample diameter (average 1.8 mm) with a gauge length of 10 mm was used and the final length after extension was 20 mm. The extension rate was set as 1 mm/min. Before each scan, clamp's load was tared after positioning the gauge using the auto-home function. Tablets which broke at the holding point were excluded from the study to rule out the artefact of power concentration at clamping point. Each measurement was recorded as the mean of four replicates.

2.9 Weight uniformity

Ten tablets were randomly selected and weighed using a Discovery DV215CD digital balance (Ohaus Corporation, USA). The average mass, standard deviation and percentage deviation from average mass were determined for each design.

2.10 **In vitro** ***drug release testing***

The impact of tablet design on the release pattern of the 3D printed tablets was assessed using a United States Pharmacopeia (USP II) dissolution test apparatus (Erweka GmbH, Germany). The dissolution test was adapted from the USP monograph for immediate release theophylline tablets (USP, 2007). The dissolution study was conducted in 900 mL of 0.1 M hydrochloric acid (pH 1.2) at 37 ± 0.5 °C and with paddle speed of 50 rpm. The amount of released theophylline was determined at 5 min intervals by UV/VIS spectrophotometer (PG Instruments Limited, UK) at the wavelength of 272 nm and path length of 1 mm. Data was analysed using IDISis software (Automated Lab, UK, 2012). The concentration of theophylline was calculated using a calibration curve of standard drug solutions in the acidic medium (concentration range: 10-250 mg/L, Linear equation: Ab=0.00535 C+0.00134, where Ab is UV absorbance and C is theophylline concentration in mg/L, and coefficient of determination R^2 = 0.9996). Each sample was tested in trilicate and in vitro release patterns of theophylline were plotted versus time using the average percentage value with error bars representing the standard deviation. In order to assess the disintegration behaviour of the 3D printed tablet during the dissolution test, the dissolution was video-recorded using a Sony HXR-NX3 camera (Sony Electronics Inc., Japan) with the macro option on. Wide-angle green laser probes were used to illuminate the tablets during dissolution in a dark room.

To assess the swelling behaviour of cellulosic matrix in the dissolution medium as well as drug diffusion pattern, real-time UV imaging for the polymeric matrix was assessed using an Actipix SDI300 dissolution imaging system (Paraytec Ltd., York, UK) with Actipix flow-through type dissolution cartridge. The sample was exposed therefore to the dissolution media through one surface only (area of 12.57mm^2). The dissolution media was flowing over the top surface using a UV filter of 280 nm. The collection of the data was achieved using SDI Online Mode software (v 1.8.50805, Paraytec Ltd, York, UK). The obtained data were analysed using SDI Offline Mode software (v1.8.50805, Paraytec Ltd, York, UK). The software allowed the conversion of the data from UV measurement into drug concertation after the input of drug's absorptivity.

2.11 Statistical analysis

One-way analysis of variance (ANOVA) was employed using SPSS Software (22.0.0.2) to analyse the differences in the percentage of drug released at T=30 min. Differences in results where $p \leq 0.05$ were considered significant, and p of >0.05 was considered not significant.

3. **Results and discussion**

As illustrated in Fig.1**,** a range of tablets with built-in gaps were engineered with the design aim of breaking rapidly upon contact with aqueous medium. The tablets were composed of 9 repeated units (blocks) that are connected together with three bridges: two at the bottom and top of the tablet and a third at the mid-level of the tablet structure. Initially, 3 sets of tablets with block widths (0.5, 1 or 1.5 mm) were designed. Each set was printed with increasing inter-block spacing: namely 0, 0.2, 0.4, 0.6, 0.8, 1.0 or 1.2 mm.

A theophylline loaded cellulosic filament processed by HME extrusion was used as a feed for FDM 3D printing to fabricate these designs. TGA data indicated minimal weight loss following the two thermal processes of HME and FDM 3D printing, and suggested that tablet contents remained stable under the processing conditions (Fig. 2A). Thermal analysis data indicated that a portion of theophylline remained in a crystalline form based on the presence of a melting peak at 258 ^{o}C **(**Fig. 2B**)**. The same DSC thermal scan also showed that the filament has a glass transition temperature (Tg) of 46 ^{o}C and was compatible with FDM 3D printing process. The additional thermal processing of the filament through a FDM 3D printer nozzle did not seem to significantly affect the Tg or the drug's melting point in the tablet **(**Fig. 2B**)**. XRD patterns of the filament and 3D printed tablets confirmed the crystalline nature of theophylline in the cellulosic matrix in both filament and 3D printed tablet (Supplementary data, Fig. S1C) with the presence of intensity peaks at 2Theta = 7 ^{o}, 12 ^{o}, 14 ^{o} and 24^{o} that are typical of theophylline crystals (Rasanen et al., 2001).

Figs. 3A and 3B show rendered images and photographs of sets of 1 mm blocks (Images of a printed set of tablets with 1.5mm width blocks are shown in Supplementary Data, Fig. S1). The use of the bridge system design allowed for a structurally stable tablet to result from and during the printing process: the lower bridge allows the building of a base for the tablet and facilitated tablet recovery upon completion of the 3D printing process. The middle and upper bridges helps the formation of coherent and easy-to-handle tablets. SEM images confirmed that the gap spaces were parallel to the blocks as envisaged in the design (Fig. 3C). However, when designs of a thinner block (0.5 mm) were printed, they yielded distorted and incomplete structures and were concluded as unsuitable. The limited resolution of FDM 3D printing (Armillotta, 2006) was the likely reason for the distortion.

The internal structure of the 3D printed tablet was assessed using XμCT technique (Fig. 4). The technique confirmed the consistent parallel blocks and spaces throughout the tablet layers. Each block was composed of 3 lines of 300 μm wide fused extrudates and were connected by three bridges at right angles to the central axis of the block. In general, the quality of the printed design were lower than what is usually achieved with FDM 3D printing. It is possible that due to the complicated nature of the design, the flow of the material is frequently interrupted with numerous stop-start orders of the moving heads. The stop-start process may have contributed to the fluctuation in the weight of printed tablet (Table 1). In addition, the shallowness of the blocks of the structure in CAD designs negates the possibility of using shell layer(s) to cover the internal core as commonly used in FDM 3D printing.

The impact of design on the mechanical properties of the constructed tablets was assessed via examining tablet crushing and tensile strength as well as friability. The material of fabrication for the 3D printed tablets is the same and in theory should have the same the hardness and disintegration time. However, the presence of weak bridges creates weak points that tend to break first in a crushing test (whilst the constituent block components remains intact). Increasing inter-block spaces led to significant reduction in tablet crushing strength ($p<0.05$). A stark difference was noted for solid tablets (without spaces), which exhibited a crushing strength of 227 N in comparison to 17 N for the 1.2 mm spaced blocks (Table 1). It is worth noting that crushing of these tablets is fundamentally different to that of tablet produced by powder compression, where cracks are initiated in the compressed tablet at defect point(s) and propagate across the tablet. In our example, the cracks occur in multiple locations at the weakest points (bridges) while the blocks remained intact.

Tensile strength examination also revealed an inverse relationship between the average maximum load at breakage of the tablets and the spacing between the tablets (Table 1). The load on the sample is likely to be eccentric due to the inconsistent nature of the structure (presence of inter-block spaces). These spaces concentrate the stress on inter-blocks bridges and subject them to lateral disturbing load. Such a trend appeared to be directly related to the length of inter-block bridges. Increasing the spaces between the blocks will reduce the structural strength hence causes the inter-blocks bridges to fail under the applied stress. However, the design impact on crushing and tensile strength of the constructed tablets did not affect tablet handling robustness, as indicated from the zero values of friability that was obtained for all designs (inter-block spaces 0-1.2 mm) of the HPC-based FDM 3D printed tablets (Table 1).

The dissolution profiles of in vitro drug release from the 3D printed tablet designs have been largely influenced by the tablet design (Fig.5A for 1 mm block set, see also Supplementary Data, Fig. S2 for 1.5 mm set). The rate of in vitro drug release was directly related to the distance between the blocks. Tablets with no or 0.2 mm spaces showed a slow drug release (<45%) after 30 min. It is worth noting that in tablets of narrow inter-block spacing (0.2 and 0.4 mm), the blocks tend to swell and a form a gel layer on the surface, this layer facilitates blocks adhesion in a random pattern. The blocks can possibly separate after a significant period of time (particularly for 0.4mm spacing) and accelerate drug release. This has resulted in relatively erratic release patterns (Fig 5A). When larger spacing was employed (≥0.6 mm), the separation of the blocks following bridge dissolution was the dominant phenomenon and yielded a more predictable release pattern. As a result, drug release was accelerated to >80% at T=30 min when the inter-block spacing was increased to 0.6 mm (Fig. 5B**).** Inter-block spaces of 1.0 or 1.2 mm were deemed necessary to meet compendial expectations for immediate release products (i.e. >85% release in 30 min). The wider the space between blocks in the tablet the less resistance to medium flow through its structure.

Numerous literature reports indicated that the dissolution of solid dispersion and crystals are directly linked to surface area/mass ratio (Armstrong and Haines-Nutt, 1973; Kubo and Mizobe, 1997; Nilkumhang et al., 2009; Zhang et al., 2014). However, tablets of inter-block spaces of >0.6 mm have only a marginal increase on surface/mass ratio over 0.2 and 0.4 mm space block tablets **(**Table 1**)**. This finding suggests that the marked acceleration of drug release when spaces are increased should not only be attributed to a slight increase in surface/mass ratio.

An insight into the mechanism responsible for accelerating drug release from 3D printed tablets can be deduced from observation of structural changes during in vitro dissolution. Fig. 6A shows the time-to-break of tablets with increasing inter-block spaces during in vitro dissolution. Tablets with 0 (solid) and 0.2 mm spaces did not break during dissolution, whilst spacing of 0.4 and 0.6 mm allowed a better ingress of the medium into inner surfaces of the blocks, causing blocks of the tablet to detach following the dissolution of the bridges. Using imaging with wide-angle laser illumination, for an inter-block spacing of 1.2 mm images showing tablets breaking into blocks in <6 min was confirmed (Fig. 6B**)**.

The interaction of the cellulosic matrix of the tablets with simulated gastric dissolution medium has been assessed using real-time UV imaging (Fig. 7A). Within the first few minutes, the

polymer matrix showed some level of expansion due to swelling of HPC upon introduction of dissolution medium. This was followed by a steady erosion of the polymeric matrix at a rate of 8µm/min **(**Fig. 7B**)**. For designs of narrower spaces (0.2-0.4 mm), it is possible that the swelling of the blocks led to further narrowing of the spaces followed by the fusion of blocks, leading to formation of a unit of joined blocks. Such a structure would thus inhibit tablet fragmentation as well as drug release in accordance with the in-vitro dissolution data presented earlier.

Erosion and swelling mechanisms have been previously reported to have major influence on drug release from an HPC matrix (Van Nguyen et al., 2016; Vueba et al., 2004). As the cellulosic polymer becomes introduced to the aqueous medium, it absorbs water starting from the surface leading to progressive polymer hydration, swelling and the formation of a viscous gelatinous layer (Korsmeyer and Peppas, 1983). While polymer erosion accelerates release rate (Sujja-areevath et al., 1998), swelling tends to retard release with the formation of viscous diffusion pathways. In this work, the introduction of gap in the tablet design would appear to have prevented the formation of a single large cellulosic matrix and accelerated drug release by both facilitating erosion as well as keeping diffusion pathways within swollen individual blocks to minimal levels.

One established approach to accelerate tablet disintegration and dissolution in aqueous medium, is through the inclusion of functional additives, disintegrants. In order to compare our design approach with the conventional disintegrant addition, several commercially available disintegrants were incorporated in the filament composition and printed using solid tablet design (no spaces) (Supplementary data, Fig. S3). The addition of the disintegrants was found to have no significant effect on in vitro theophylline drug release from the FDM constructed tablets. It is worth reporting that even a further increase in disintegrant level to 10% (w/w) did not result in any disintegration effect or acceleration in dissolution rate of the printed tablets. This finding of no enhancement was attributed in part to the mechanism of action of these disintegrants, which facilitate disintegration via swelling (Alebiowu and Itiola, 2003) and wicking (Kissa, 1996) within a compressed powder structure to increase the internal pressure and accelerate the dosage form to fall apart. It was also noted that crospovidone may also cause disintegration by a shape recovery mechanism upon wetting (Desai et al., 2012). Given the intimate mixing that occurs during HME and FDM 3D printing, such disintegration mechanisms appear to be greatly disrupted by the thermal processing of disintegrant particles with softened/molten polymers.

The use of a design approach to enhance the speed of release from an excipient-rich matrix, commonly produced via 3D printing technologies, has also been recently reported using a tablet design with perforated channels (Sadia et al., 2018) or multi-chamber structure (Kyobula et al., 2017). Employing design approaches to these systems, means that widely differing release rate functionality can be achieved from a single formulation and obviates the need to use different formulations to achieve different release rates. This benefit comes with significant cost savings.

4. Conclusions

An innovative tablet design approach to include built-in gaps in the 3D printed tablet architecture has been demonstrated. The unique tablet design is based on the construction of a capsule-shaped tablet with multiple interconnected blocks. Upon introduction to dissolution medium, the tablets demonstrated a unique ability to break into mini-structures hence accelerating drug release in comparison to solid non-gap-containing 3D printed tablets. A range of design attributes were investigated. An inter-block spacing of 1.0 mm was deemed necessary for the drug release profile to meet the pharmacopeial criteria of immediate release products. The above design was superior to a more conventional formulation approach of including disintegrants in 3D tablets to achieve rapid disintegration and dissolution. The innovative approach allows one to craft an immediate release cellulosic tablet with substantial drug dose. This work also illustrates the potential of employing computer-aided design to construct tablets of complex geometries and modify their in vitro performance to meet the mechanical and functional expectations of a traditional pharmaceutical product. Whilst the authors have shown the potential utility of the design for oral administration, the incorporation of a multi-block design can be adopted in the designs of implants or stents where enhancing the release rate of an eluting drug from rich polymeric structures is also needed.

Acknowledgments

The authors would like to thank UCLan Innovation Team for this support and Mrs Reem Arafat for her help with graphics design. The authors would also like to acknowledge the School of Medicine and Biomedical Sciences, Sheffield University for their support with XμCT data.

Conflicts of interest M A Alhnan is the innovator in patent applications WO 2016038356 A1, WO2017072536A1 and WO2018020237A1 in the field of 3D printing of medicines.

References

Alebiowu, G., Itiola, O.A., 2003. Effects of starches on the mechanical properties of paracetamol tablet formulations. II. Sorghum and plantain starches as disintegrants. Acta Pharm 53, 313-320.

Alhnan, M.A., Okwuosa, T.C., Sadia, M., Wan, K.-W., Ahmed, W., Arafat, B., 2016. Emergence of 3D Printed Dosage Forms: Opportunities and Challenges. Pharm Res 33, 1817-1832.

Armillotta, A., 2006. Assessment of surface quality on textured FDM prototypes. Rapid Prototyping J 12, 35-41.

Armstrong, N.A., Haines-Nutt, R.F., 1973. Proceedings: Dissolution rate and the surface area of compacted powder systems. J Pharm Pharmacol 25, Suppl:147P.

Desai, P.M., Liew, C.V., Heng, P.W., 2012. Understanding disintegrant action by visualization. J Pharm Sci 101, 2155-2164.

GBIResearch, 2012. Oral drug delivery market report, last accessed 27/2/2018, available from: http://www.contractpharma.com/issues/2012-06/view_features/oral-drug-delivery-market-report/.

Goole, J., Amighi, K., 2016. 3D printing in pharmaceutics: A new tool for designing customized drug delivery systems. Int J Pharm 499, 376-394.

Goyanes, A., Buanz, A.B.M., Basit, A.W., Gaisford, S., 2014. Fused-filament 3D printing (3DP) for fabrication of tablets. Int J Pharm 476, 88-92.

Goyanes, A., Fina, F., Martorana, A., Sedough, D., Gaisford, S., Basit, A.W., 2017. Development of modified release 3D printed tablets (printlets) with pharmaceutical excipients using additive manufacturing. Int J Pharm 527, 21-30.

Goyanes, A., Robles Martinez, P., Buanz, A., Basit, A.W., Gaisford, S., 2015. Effect of geometry on drug release from 3D printed tablets. Int J Pharm 494, 657-663.

Kissa, E., 1996. Wetting and wicking. Text Res J 66, 660-668.

Korsmeyer, R.W., Peppas, N.A., 1983. Macromolecular and modelling aspects of swelling-controlled systems, in: Roseman, T.J., Mansdorf, S.Z. (Eds.), Controlled Release Delivery Systems. Marcel Dekker, New York, pp. 77-90.

Kubo, H., Mizobe, M., 1997. Improvement of dissolution rate and oral bioavailability of a sparingly water-soluble drug, (+/-)-5-[[2-(2-naphthalenylmethyl)-5-benzoxazolyl]-methyl]- 2, 4-thiazolidinedione, in co-ground mixture with D-mannitol. Biol Pharm Bull 20, 460-463.

Kyobula, M., Adedeji, A., Alexander, M.R., Saleh, E., Wildman, R., Ashcroft, I., Gellert, P.R., Roberts, C.J., 2017. 3D inkjet printing of tablets exploiting bespoke complex geometries for controlled and tuneable drug release. J Control Release 261, 207-215.

Lam, C.X.F., Mo, X.M., Teoh, S.H., Hutmacher, D.W., 2002. Scaffold development using 3D printing with a starch-based polymer. Mater Sci Eng C-Biomimetic and Supramolecular Systems 20, 49-56.

Marketsandmarkets, 2013. Drug delivery technology market, last accessed 27/2/2018, available from: https://www.marketsandmarkets.com/Market-Reports/drug-delivery-technologies-market-1085.html?gclid=CIXRuMT5osQCFe6WtAodmiUAZg

Nilkumhang, S., Alhnan, M.A., McConnell, E.L., Basit, A.W., 2009. Drug distribution in enteric microparticles. Int J Pharm 379, 1-8.

Okwuosa, T.C., Stefaniak, D., Arafat, B., Isreb, A., Wan, K.W., Alhnan, M.A., 2016. A Lower Temperature FDM 3D Printing for the Manufacture of Patient-Specific Immediate Release Tablets. Pharm Res 33, 2704-2712.

Rasanen, E., Rantanen, J., Jorgensen, A., Karjalainen, M., Paakkari, T., Yliruusi, J., 2001. Novel identification of pseudopolymorphic changes of theophylline during wet granulation using near infrared spectroscopy. J Pharm Sci 90, 389-396.
Rowe, C.W., Katstra, W.E., Palazzolo, R.D., Giritlioglu, B., Teung, P., Cima, M.J., 2000. Multimechanism oral dosage forms fabricated by three dimensional printing. J Control Release 66, 11-17.
Sadia, M., Arafat, B., Ahmed, W., Forbes, R.T., Alhnan, M.A., 2018. Channelled tablets: An innovative approach to accelerating drug release from 3D printed tablets. J Control Release 269, 355-363.
Sadia, M., Sosnicka, A., Arafat, B., Isreb, A., Ahmed, W., Kelarakis, A., Alhnan, M.A., 2016. Adaptation of pharmaceutical excipients to FDM 3D printing for the fabrication of patient-tailored immediate release tablets. Int J Pharm 513, 659-668.
Skowyra, J., Pietrzak, K., Alhnan, M.A., 2015. Fabrication of extended-release patient-tailored prednisolone tablets via fused deposition modelling (FDM) 3D printing. Eur J Pharm Sci 68, 11-17.
Sujja-areevath, J., Munday, D.L., Cox, P.J., Khan, K.A., 1998. Relationship between swelling, erosion and drug release in hydrophilic natural gum mini-matrix formulations. European Journal of Pharmaceutical Sciences 6, 207-217.
Sun, Y., Soh, S., 2015. Printing Tablets with Fully Customizable Release Profiles for Personalized Medicine. Adv Mater 27, 7847-7853.
Tagami, T., Fukushige, K., Ogawa, E., Hayashi, N., Ozeki, T., 2017. 3D Printing Factors Important for the Fabrication of Polyvinylalcohol Filament-Based Tablets. Biol Pharm Bull 40, 357-364.
USP, 2007. The United States Pharmacopeia: USP29: Dissolution monograph for theophylline tablets. United States Pharmacopeial Convention Inc., Rockville, MD.
Van Nguyen, H., Nguyen, V.H., Lee, B.J., 2016. Dual release and molecular mechanism of bilayered aceclofenac tablet using polymer mixture. Int J Pharm 515, 233-244.
Vueba, M.L., Batista de Carvalho, L.A., Veiga, F., Sousa, J.J., Pina, M.E., 2004. Influence of cellulose ether polymers on ketoprofen release from hydrophilic matrix tablets. Eur J Pharm Biopharm 58, 51-59.
Zhang, J., Yang, W., Vo, A.Q., Feng, X., Ye, X., Kim, D.W., Repka, M.A., 2017. Hydroxypropyl methylcellulose-based controlled release dosage by melt extrusion and 3D printing: Structure and drug release correlation. Carbohydr Polym 177, 49-57.
Zhang, Y., Che, E., Zhang, M., Sun, B., Gao, J., Han, J., Song, Y., 2014. Increasing the dissolution rate and oral bioavailability of the poorly water-soluble drug valsartan using novel hierarchical porous carbon monoliths. Int J Pharm 473, 375-383.

List of Figures

Fig 1. Schematic illustration showing concept of multi-block unit in comparison with an equivalent non-block design. **(A)** Rendered image of solid tablet (joining 9 blocks without spaces, control). **(B)** The novel design is based on 9 repeating units (blocks) joined together by 3 bridges. The capsule-like general shape was maintained by using curved side units. **(C)** Three sets of tablets were printed with a different block size (0.5, 1 and 1.5 mm). Each set were designed with increasing spaces: 0, 0.2, 0.4, 0.6, 0.8, 1.0 and 1.2 mm.

Fig. 2. Thermal and X-Ray powder diffraction analysis of theophylline loaded filament and 3D printed tablets. **(A)** Thermal degradation profile, **(B,C)** DSC thermograph (second heating cycle) and X-Ray Powder diffraction spectra of theophylline, HPC SSL, physical mixture of theophylline and HPC, Extruded filament of theophylline and HPC SSL, tablet of theophylline and HPC.

Fig. 3. A) Rendered images and **B)** photographic images of tablet designs with 1 mm block and increasing inter-block spacing: 0, 0.2, 0.4, 0.6, 0.8, 1.0 and 1.2 mm. **C)** SEM images of inter-channel spaces for these tablets.

Fig. 4. Visualisation of XμCT data of the internal structure of the 3D printed tablets (1mm block with 1.2 spaces). View from the **(A)** side, **(B)** bottom, (**C1, C2)** X-Y sections across the 3D printed tablets showing **(C1)** upper and **(C2)** middle bridge.

Fig. 5. (A) Impact of space distance on in vitro theophylline release into gastric medium from 3D printed tablets (1 mm block) with increasing spaces (0, 0.2, 0.4, 0.6, 0.8, 1.0 and 1.2 mm). **(B)** Drug release (%) after 30 min of dissolution test (USP II paddle 50 rpm, 37 ^{o}C, n = 3)

Fig. 6. (A) Average time-to-break for tablets during USP II dissolution test in gastric medium (USP II paddle 50 rpm, 37 ^{o}C, n = 3). Wide angle laser imaging during the first 10 min of USP II dissolution test of 3D printed theophylline tablets with **(B1)** solid tablet design, **(B2)** 3D printed tablet design (1 mm block with 1.2 mm spaces).

Fig. 7. UV imaging of in vitro dissolution of theophylline at 272 nm from 3D printed tablet vertically positioned in flow-through cell in gastric medium (0.1 M hydrochloric acid, pH 1.2). UV images (absorbance) obtained **(A1)** immediately upon filling of the cell t = 1 min and **(A2)** after the flow of dissolution medium (t = 30 min), **(B1)** cut-off from profile tracking on Z-axis during 30 min of the dissolution process. **(B2)** the erosion of 3D printed tablet during dissolution as measured by changes in the height of iso-absorbance band.

List of tables

Table 1. Spaces of CAD design, dimensions, volume, surface area, surface area/volume ratio of the CAD design, surface area/average mass ratio, maximum load and crushing strength of the 3D printed tablets (1 mm block)..

Supplementary data

Fig. S1. A) Rendered images and **B)** photographic images of tablet designs with **1.5 mm block** and increasing inter-block spacing: 0, 0.2, 0.4, 0.6, 0.8, 1.0 and 1.2 mm.

Fig. S2. Impact of space distance on in vitro theophylline release into gastric medium from 3D printed tablets (1.5 mm block) with increasing spaces (0, 0.2, 0.4, 0.6, 0.8, 1.0 and 1.2 mm).

Fig. S3. Rendered image **(A1)** photographic image **(A2)** of solid tablet (control). **(B)** SEM images of the two joint blocks. **(C)** Impact of integrating disintegrant on drug release from solid tablet (control).

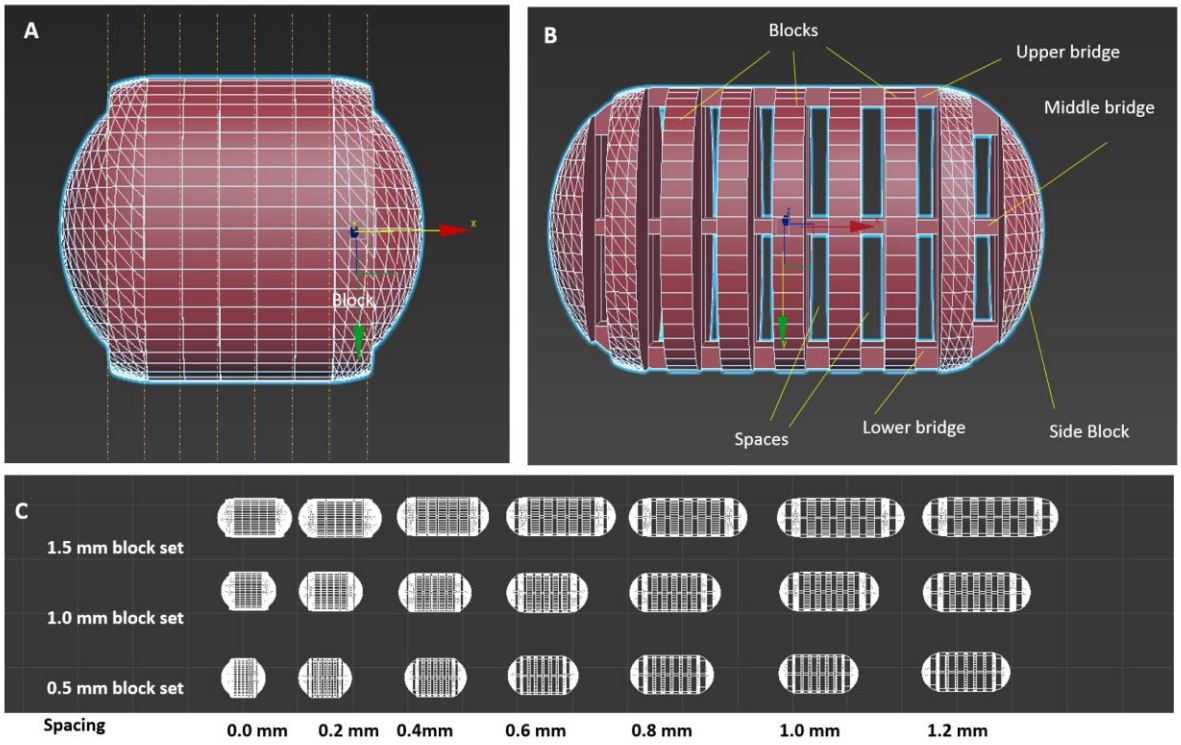

Fig 1. Schematic illustration showing concept of multi-block unit in comparison with an equivalent non-block design. **(A)** Rendered image of solid tablet (joining 9 blocks without spaces, control). **(B)** The novel design is based on 9 repeating units (blocks) joined together by 3 bridges. The capsule-like general shape was maintained by using curved side units. **(C)** Three sets of tablets were printed with a different block size (0.5, 1 and 1.5 mm). Each set were designed with increasing spaces: 0, 0.2, 0.4, 0.6, 0.8, 1.0 and 1.2 mm.

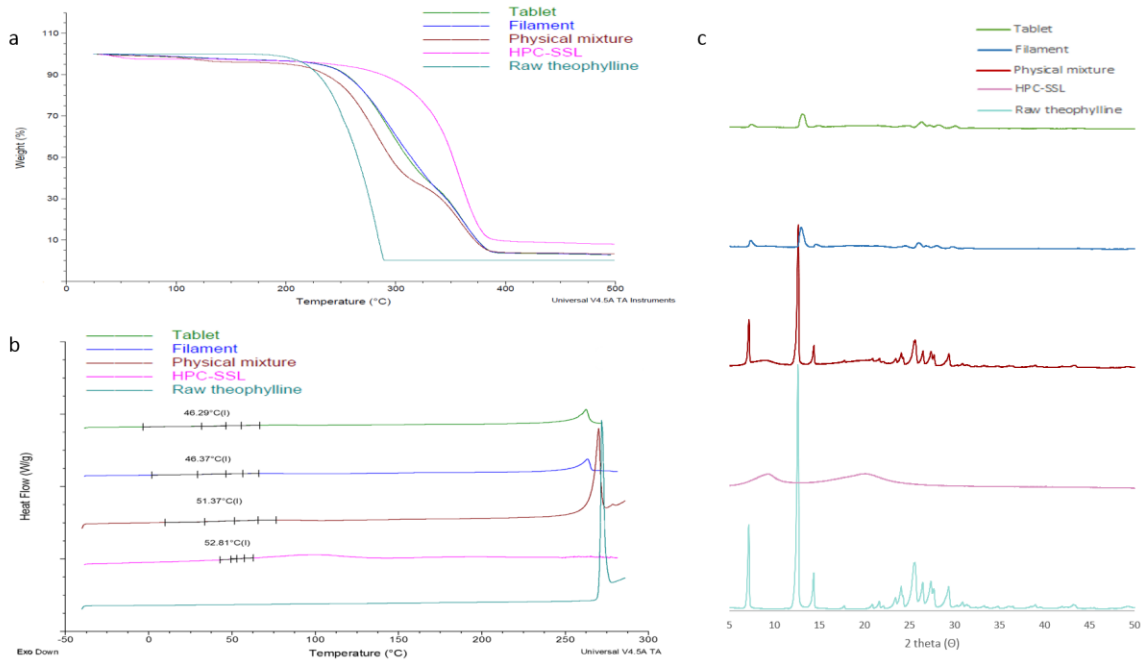

Fig. 2. Thermal and X-Ray powder diffraction analysis of theophylline loaded filament and 3D printed tablets. **(A)** Thermal degradation profile, **(B,C)** DSC thermograph (second heating cycle) and X-Ray Powder diffraction spectra of theophylline, HPC SSL, physical mixture of theophylline and HPC, Extruded filament of theophylline and HPC SSL, tablet of theophylline and HPC.

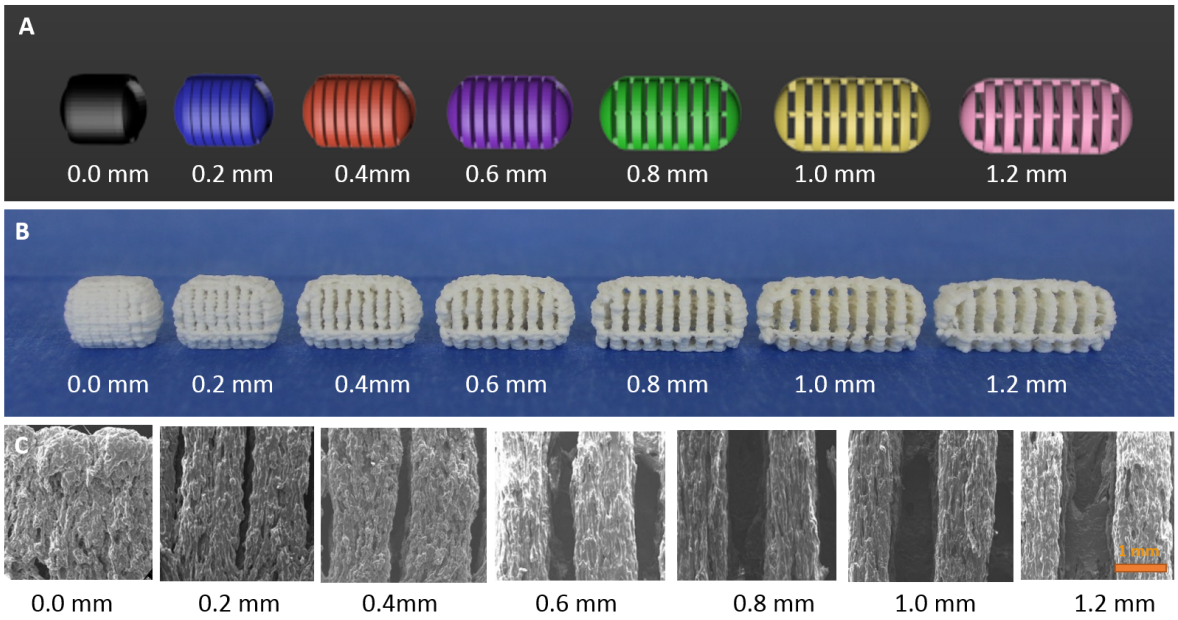

Fig. 3. A) Rendered images and **B)** photographic images of tablet designs with 1 mm block and increasing inter-block spacing: 0, 0.2, 0.4, 0.6, 0.8, 1.0 and 1.2 mm. **C)** SEM images of inter-channel spaces for these tablets.

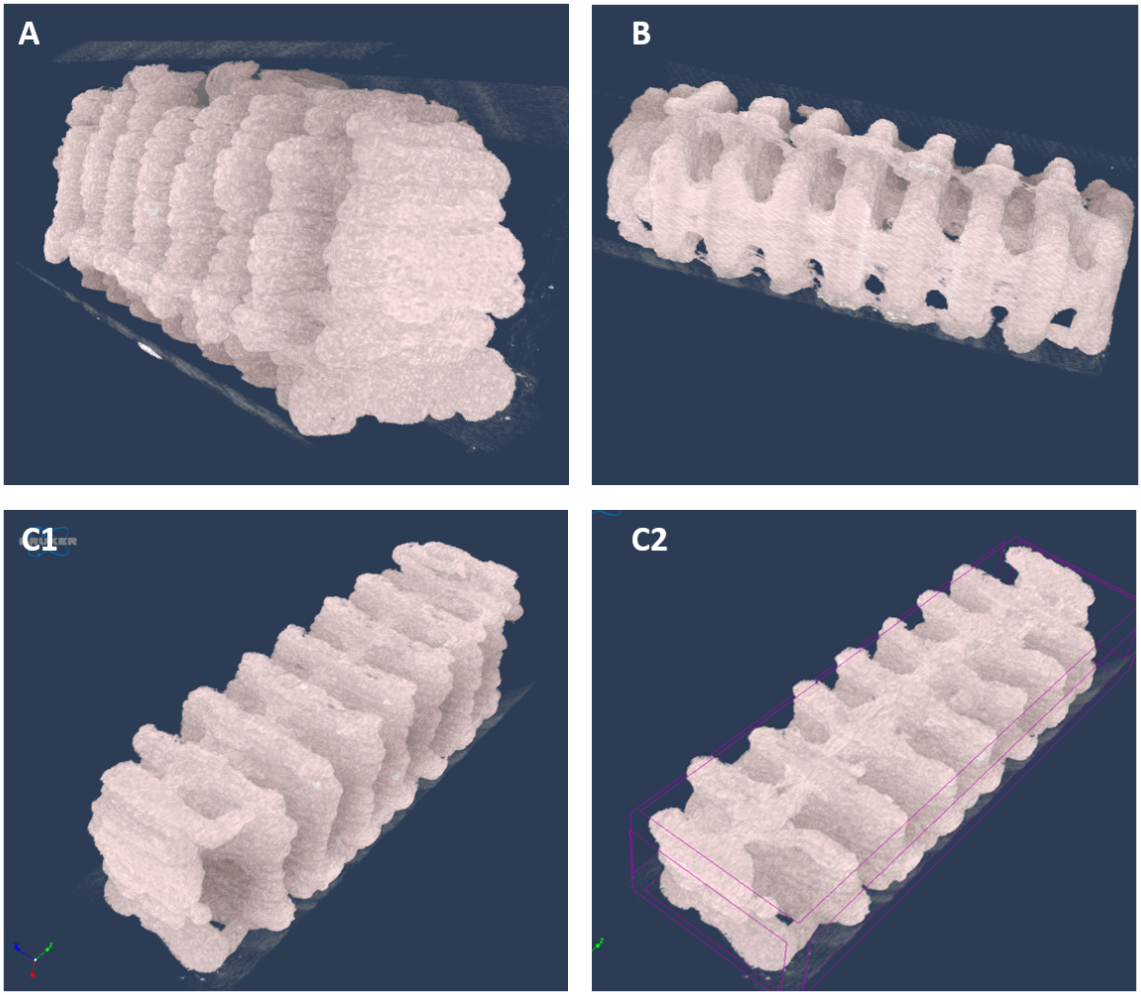

Fig. 4. Visualisation of XμCT data of the internal structure of the 3D printed tablets (1mm block with 1.2 spaces). View from the **(A)** side, **(B)** bottom, (**C1, C2)** X-Y sections across the 3D printed tablets showing **(C1)** upper and **(C2)** middle bridge.

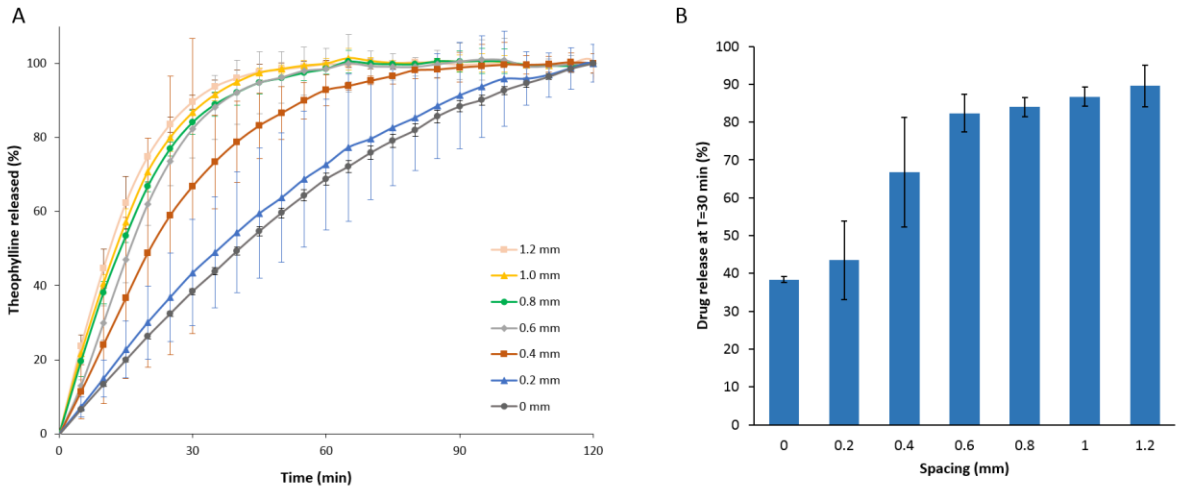

Fig. 5. (A) Impact of space distance on in vitro theophylline release into gastric medium from 3D printed tablets (1 mm block) with increasing spaces (0, 0.2, 0.4, 0.6, 0.8, 1.0 and 1.2 mm). **(B)** Drug release (%) after 30 min of dissolution test (USP II paddle 50 rpm, 37 ^{o}C, n = 3)

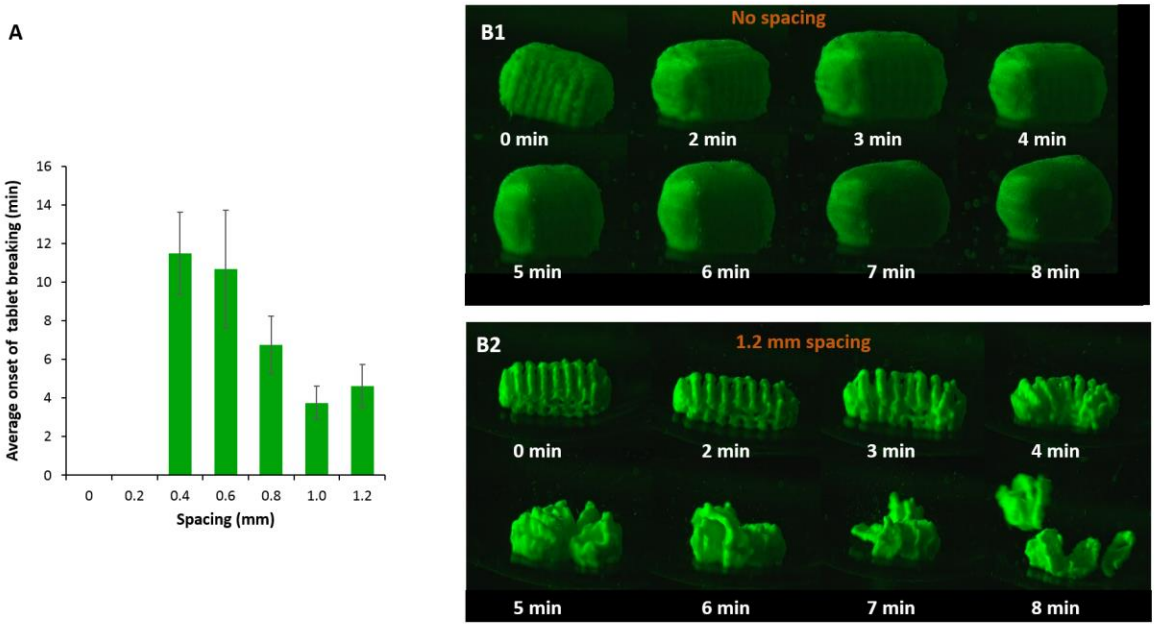

Fig. 6. (A) Average time-to-break for tablets during USP II dissolution test in gastric medium (USP II paddle 50 rpm, 37 ºC, n = 3). Wide angle laser imaging during the first 10 min of USP II dissolution test of 3D printed theophylline tablets with **(B1)** solid tablet design, **(B2)** 3D printed tablet design (1 mm block with 1.2 mm spaces).

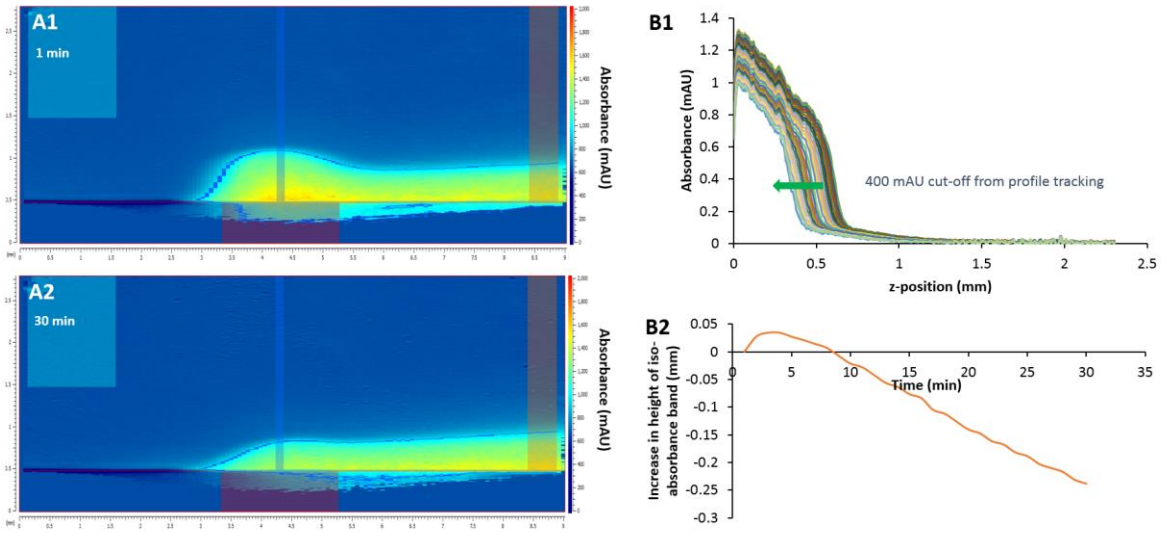

Fig. 7. UV imaging of in vitro dissolution of theophylline at 272 nm from 3D printed tablet vertically positioned in flow-through cell in gastric medium (0.1 M hydrochloric acid, pH 1.2). UV images (absorbance) obtained **(A1)** immediately upon filling of the cell t = 1 min and **(A2)** after the flow of dissolution medium (t = 30 min), **(B1)** cut-off from profile tracking on Z-axis during 30 min of the dissolution process. **(B2)** the erosion of 3D printed tablet during dissolution as measured by changes in the height of iso-absorbance band.

Table 1. Spaces of CAD design, dimensions, volume, surface area, surface area/volume ratio of the CAD design, surface area/average mass ratio, maximum load and crushing strength of the 3D printed tablets (1 mm block).

Spaces of CAD design (mm)	**Dimensions of CAD design (mm)**			**Volume of CAD design (mm^3)**	**Surface area of CAD design (mm^2)**	**Design surface area/volume ratio of CAD design (mm^{-1})**	**Tablet mass**		**Surface area/ mass ratio (mm^2/mg)**	**Maximum load (N) ±SD**	**Crushing strength (N) ±SD**
	L	**W**	**H**				**Average mass (mg) ±SD**	**SD%**			
0.0	9.9	6.6	7.1	326.7	824.4	2.52	321.9±24.3	7.51	2.55	252.9±27.5	227.5±43.5
0.2	11.5	6.6	7.1	329.0	840.0	2.65	320.56±26.2	8.18	2.62	159.9±34.5	135±48.2
0.4	13.2	6.6	7.1	331.8	852.3	2.57	316.77±21.5	6.80	2.69	151.2±44.7	77.5±22.3
0.6	14.7	6.6	7.1	334.4	864.3	2.58	326.86±1	3.68	2.64	109.6±7.7	53.6±12
0.8	16.5	6.6	7.1	337.5	879.4	2.61	325.10±12.7	3.90	2.71	63.9±12.1	37.9±8.3
1.0	18.0	6.6	7.1	339.9	893.5	2.63	337.29±16.2	4.80	2.65	25.8±12.6	25.2±2
1.2	19.5	6.6	7.1	342.3	907.4	2.65	341.89±19.8	5.80	2.65	18.6±11.3	16.7±2.6

Tablet Fragmentation without a Disintegrant: A Novel Design Approach for Accelerating Disintegration and Drug Release from 3D Printed Cellulosic Tablets

Supplementary data

Basel Arafat[1,2], Magdalena Wojsz[1,3], Abdullah Isreb[1], Mohammad Isreb[4], Waqar Ahmed[5], Tawfiq Arafat[6], Robert T Forbes[1], Mohamed A Alhnan[1]*

[1] School of Pharmacy and Biomedical Sciences, University of Central Lancashire, Preston, Lancashire, UK

[2]Department, Medicine and Healthcare Science, Anglia Ruskin University

[3]Faculty of Pharmacy with the Laboratory Medicine Division, Medical University of Warsaw, Warsaw, Poland

[4]School of Pharmacy, University of Bradford, Richmond Road, Bradford, UK

[5] College of Science/School of Mathematics and Physics, University of Lincoln, Brayford Pool, Lincoln, Lincolnshire, UK

[6] Faculty of Pharmacy and medical Sciences, Petra University, Amman, Jordan

*Corresponding author: MAlbedAlhnan@uclan.ac.uk

University of Central Lancashire, MB025 Maudland Building, Preston PR1 2HE, UK

Tel: +44 (0)1772 893590, Fax: +44 (0)1772 892929

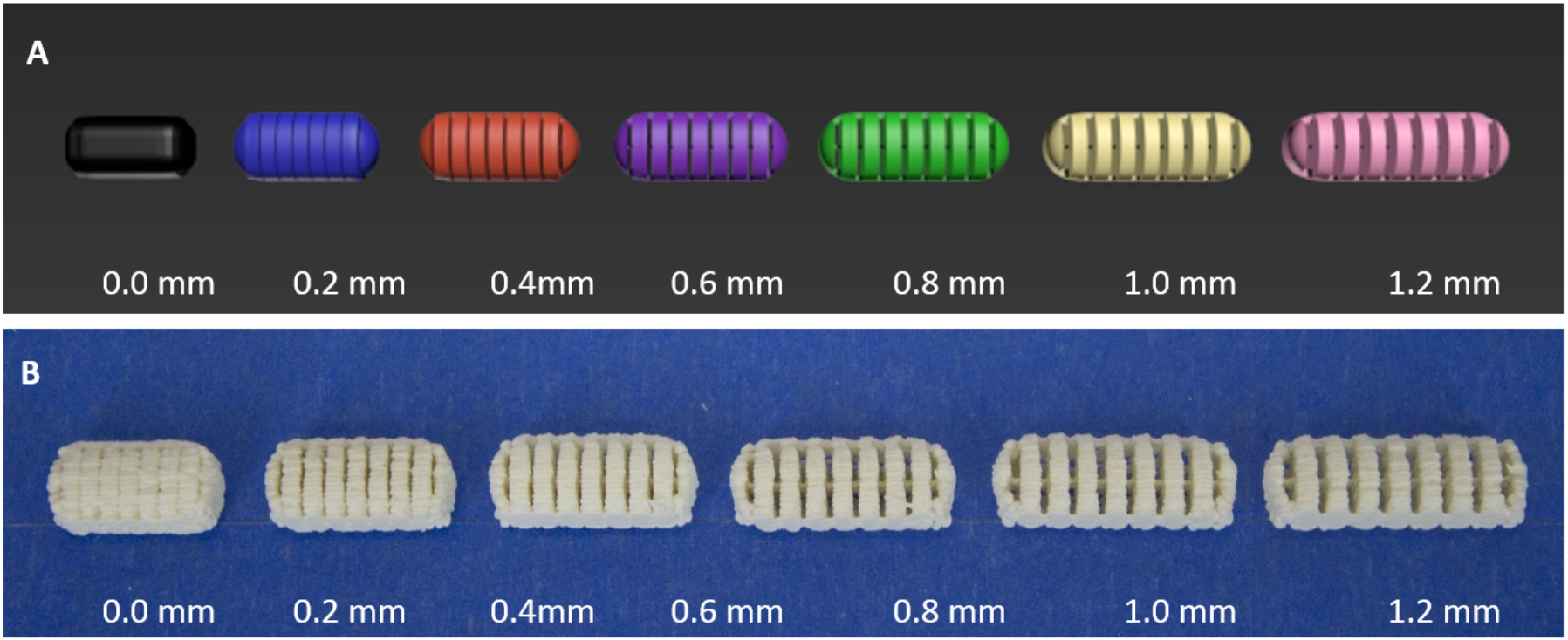

Fig. S1. A) Rendered images and **B)** photographic images of tablet designs with **1.5 mm block** and increasing inter-block spacing: 0, 0.2, 0.4, 0.6, 0.8, 1.0 and 1.2 mm.

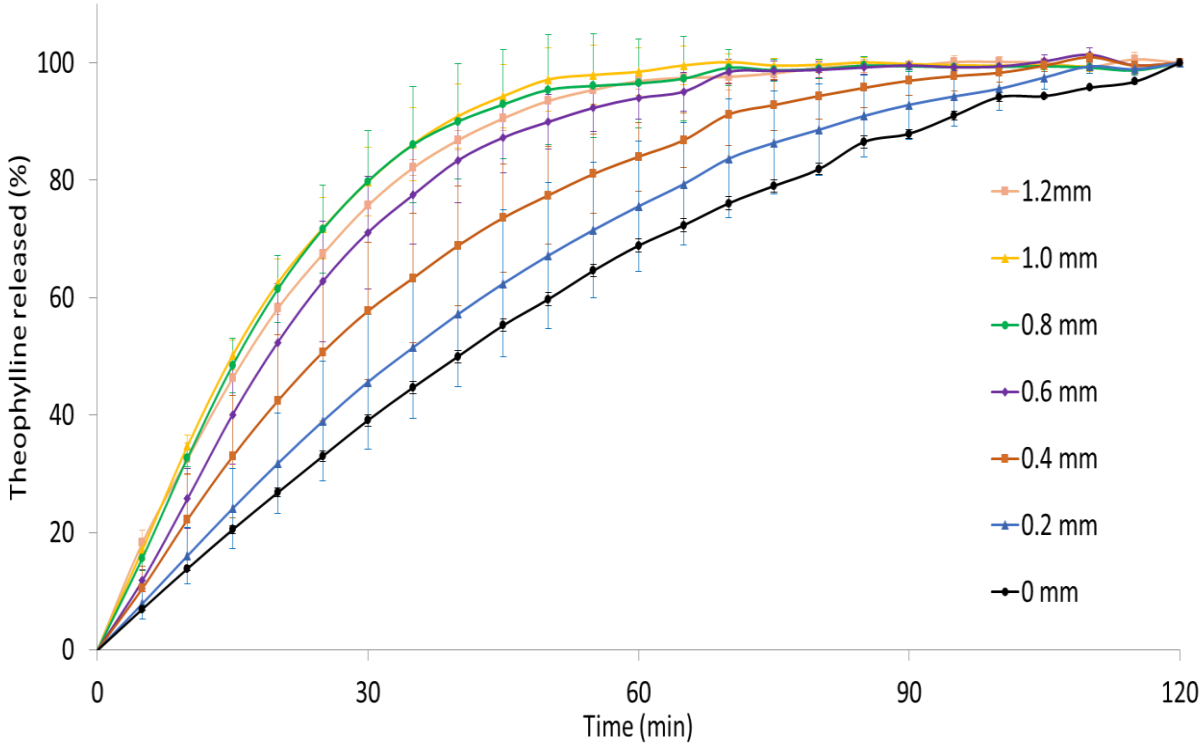

Figure S2. (A) Impact of space distance on *in vitro* theophylline release to gastric medium from 3D printed tablets **(1.5 mm block)** with increasing spaces (0, 0.2, 0.4, 0.6, 0.8, 1.0 and 1.2 mm).

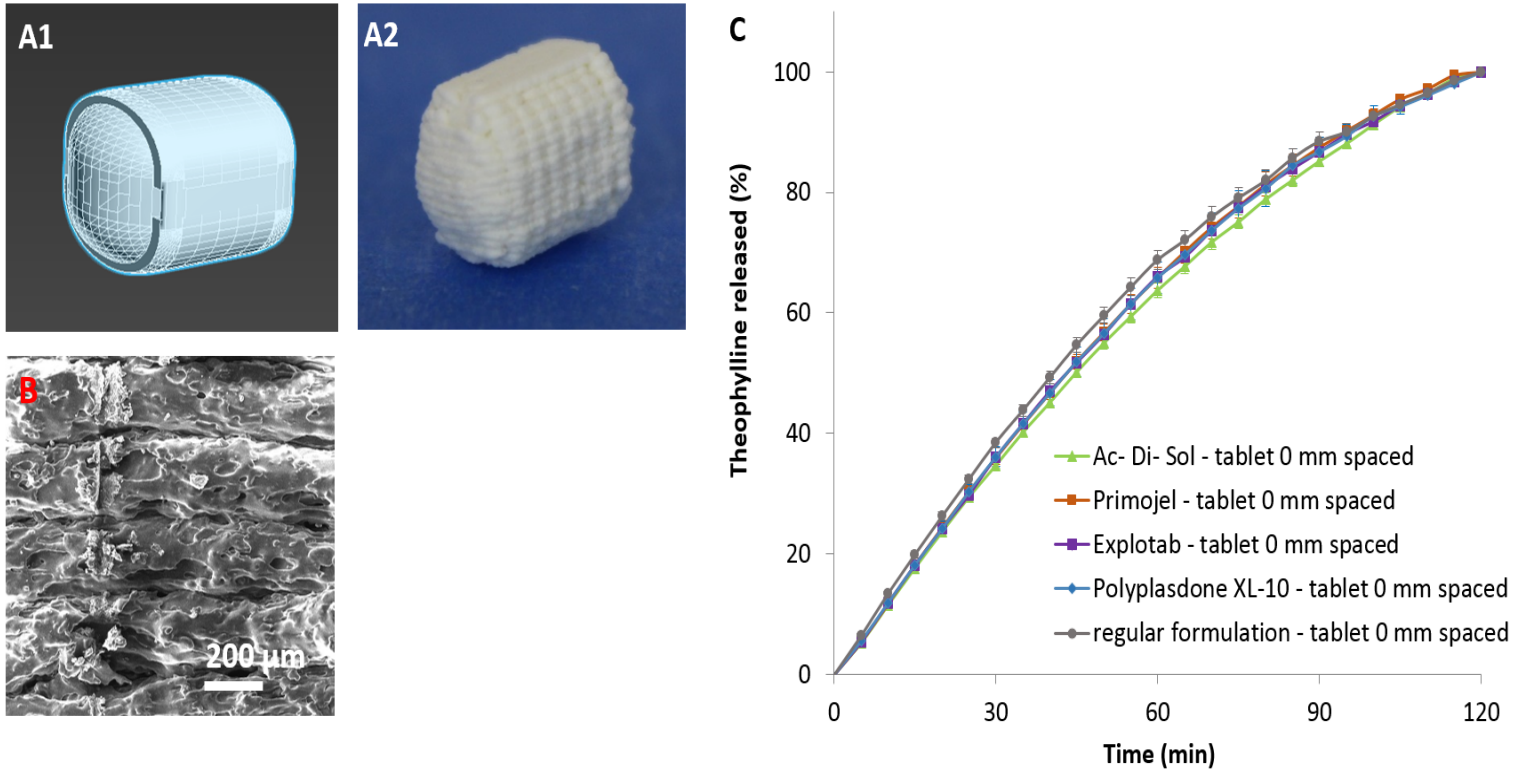

Figure S3. Rendered image **(A1)** photographic image **(A2)** of solid tablet (control). **(B)** SEM images of the two joint blocks. **(C)** Impact of integrating disintegrant on drug release from solid tablet (control).